Macromolecules
COMMUNICATION TO THE EDITOR

Macromolecules **2009**, *42*, 7251–7253 **7251**
DOI: 10.1021/ma9015888

Preparation and Characterization of Shape Memory Elastomeric Composites

Xiaofan Luo and Patrick T. Mather*

Syracuse Biomaterials Institute and Department of Biomedical and Chemical Engineering, Syracuse University, Syracuse, New York 13244

Received July 20, 2009
Revised Manuscript Received September 2, 2009

Shape memory polymers (SMPs) are a class of smart polymeric materials that have the ability to "memorize" a permanent shape, be manipulated to retain or "fix" a temporary shape, and later recover to its original (permanent) shape upon a stimulus such as heat, electricity, or irradiation.[1−3] A large number of SMPs have been developed and utilized for actuators, deployable medical devices, smart adhesives, and sensors, among others. However, very few of the existing SMPs are soft and elastomeric at the application temperature, although the demand for soft actuators is evident.[4] Three existing examples we are aware of include a main-chain liquid crystalline elastomer (LCE),[5] EPDM ionomers incorporating a range of crystallizable fatty acid salts,[6] and hydrogels with crystallizable alkyl side chains.[7] Each case involved some custom synthesis that presents inherent challenges to utilization at large scale. Here we report the development of a unique shape memory elastomeric composite (SMEC) using a new and broadly applicable approach, which involves an interpenetrating combination of a crystallizable thermoplastic microfiber network (functioning as the "switch phase" for shape memory) with an elastomeric matrix.

Our SMEC is composed of two commercially available polymers—a silicone rubber (Sylgard 184 from Dow Corning; hereafter "Sylgard") and poly(ε-caprolactone) (PCL; M_w = 65 000 g/mol from Aldrich)—and fabricated via a two-step process shown in Scheme 1. PCL was first electrospun from a 15 wt % chloroform/DMF (volume ratio = 8:2) solution (voltage = 15 kV, flow rate = 1 mL/h). The resulting nonwoven fiber mat (thickness = 0.5 mm) was then immersed in a two-part mixture of Sylgard 184 (mixing ratio = 10:1) and vacuum (30 in.Hg) was applied for 20 min to ensure complete infiltration of Sylgard 184 into the PCL fiber mat. After carefully removing the extra Sylgard 184 resin on the surface with a spatula, the infiltrated Sylgard/PCL was cured at room temperature for >48 h. The Sylgard/PCL composites fabricated showed an average PCL weight fraction (measured gravimetrically) of 25.6% (or a volume fraction of 23.6%, calculated using the densities of PCL (1.145 g/cm^3) and Sylgard (1.03 g/cm^3)) with a small standard deviation of 0.5% (sample size = 5), indicating good reproducibility of this method.

The morphology of the Sylgard/PCL composite was studied by scanning electron microscopy (SEM). The surfaces of the as spun PCL fiber mat (fiber diameter = 1.93 ± 0.60 μm; see analysis method in Supporting Information) and Sylgard/PCL composite (Figure 1a,b) clearly show that the infiltration was complete with all the original voids occupied by Sylgard 184, while the fiber structures were preserved. The static water contact angle of Sylgard/PCL composite was measured to be 104.3° (Rame-Hart 250-F1 standard goniometer), slightly higher than neat Sylgard (103.4°) and much lower than as-spun PCL (123.9°). This indicates that the Sylgard/PCL composite has a medium hydrophobic surface similar to neat Sylgard. The fractured surface of Sylgard/PCL (Figure 1c−e) further confirms the biphasic, nonwoven fiber/matrix bulk morphology. Materials of similar morphologies have been reported before for high-strength nanocomposites[8,9] and fuel cell membranes[10] but never designed for shape memory applications. In our SMEC system, it was anticipated that the elastomeric matrix (Sylgard 184) would provide rubber elasticity while the PCL microfibers would serve as a reversible "switch phase" for shape fixing (via crystallization) and shape recovery (via melting). This approach would be advantageous over the recently reported method of directly blending a semicrystalline polymer with an elastomer.[11] In the case of direct blending, the shape fixing is poor when the elastomer forms the matrix, since the semicrystalline polymer can only exist as discrete spherical particles and cannot effectively bear the load as a whole to resist the entropically driven recovery of the elastomer matrix. In our case, the percolating fiber structure results in a much larger large interfacial area which facilitates load transferring and load distribution; therefore, the shape fixing can potentially be enhanced.

The thermal and mechanical properties of the Sylgard/PCL composite were characterized using differential scanning calorimetry (DSC) and dynamic mechanical analysis (DMA). As expected, the PCL microfibers in the Sylgard/PCL composite maintain the melting and crystallization behavior similar to the bulk (DSC results available in Supporting Information). In the case of DMA (1 Hz, 3 °C/min), the tensile storage modulus (E') and tensile loss tangent (tan δ) of Sylgard/PCL composite display three distinct transitions in the given temperature range (Figure 2a,b), which can be attributed to the glass transition of Sylgard (−114.4 °C), the glass transition of PCL (−49.5 °C), and the melting of PCL (60.6 °C). All of the transition temperatures were determined from the onsets of storage modulus drop. In contrast, neat Sylgard has only two transitions: a glass transition at −115.2 °C and a minor transition at −46.9 °C associated with the melting of crystals formed during subambient cooling.[12] The Sylgard/PCL composite has a room temperature (25 °C) elastic modulus of 7.6 MPa and a low tan δ value of 0.067, indicating that the material is both soft and elastic. The stress−strain response to large deformations was studied and indicates elastomer-like behavior (Supporting Information), though with significant hysteresis due to plastic deformation of the PCL phase at room temperature. The storage modulus of the composite drops to 0.2 MPa above the melting temperature of PCL, lower than that of neat Sylgard (1.0 MPa) since PCL, at that point, is a viscous liquid with negligible contribution to overall load bearing of what is effectively a silicone foam. Such PCL melting was then utilized to impart shape memory to the Sylgard/PCL system.

The shape memory behavior was characterized by a well-established four-step thermomechanical cycling method conducted using a dynamic mechanical analyzer (Q800 DMA, TA Instruments; Figure 3a).[1,2,5,13−15] The Sylgard/PCL sample (a rectangular film; 5.17 mm × 3.13 mm × 0.56 mm) was first

*To whom correspondence should be addressed: e-mail ptmather@syr.edu; Tel (315) 443-8760; Fax (315) 443-9175.

Published on Web 09/10/2009

Scheme 1. Two-Step Fabrication of Sylgard/PCL Shape Memory Elastomeric Composites (SMECs)[a]

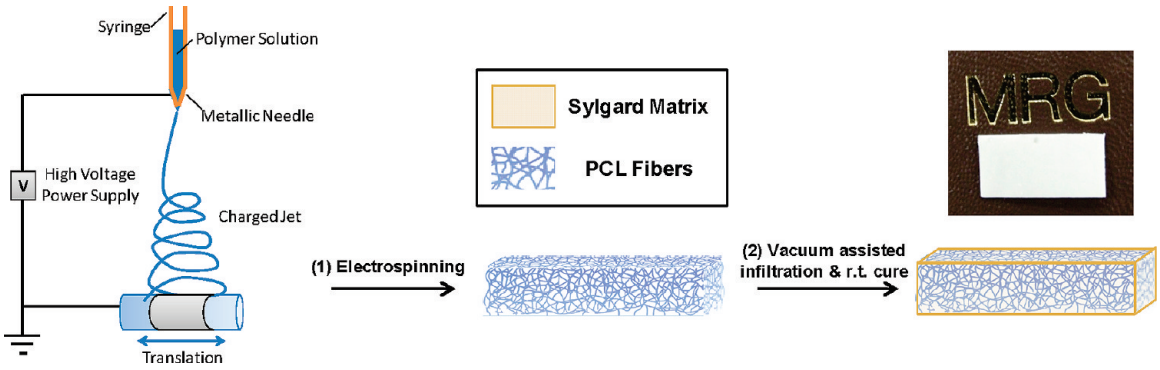

[a] The photograph (inset) shows a fully cured Sylgard/PCL sample.

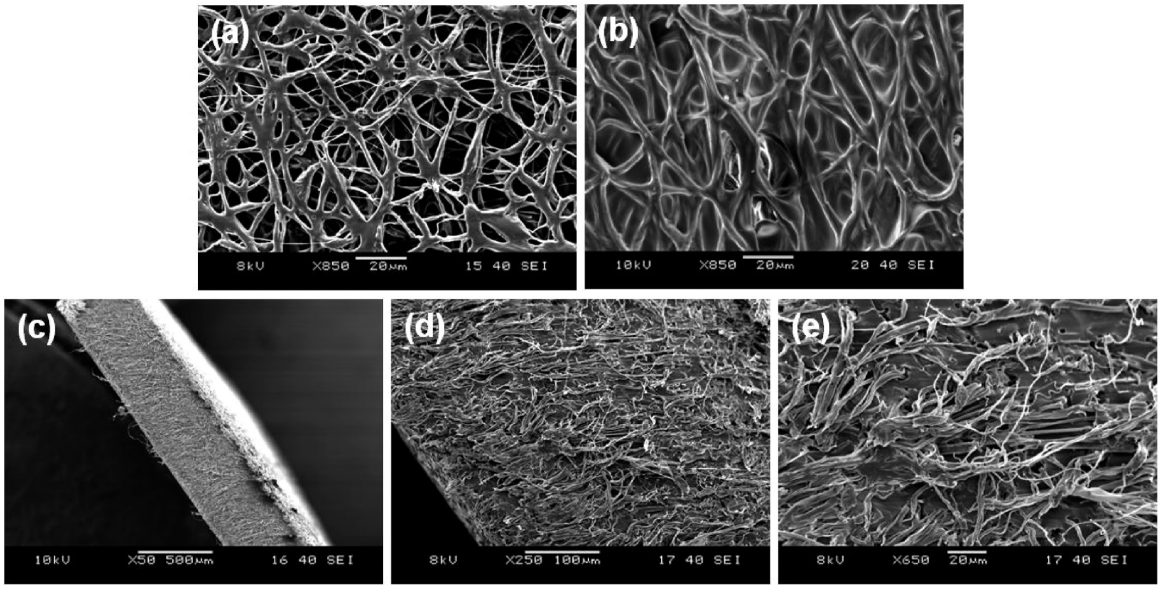

Figure 1. Scanning electron microscope (SEM) images showing (a) the surface of as-spun PCL fiber mat, (b) the surface of Sylgard/PCL composite, and (c−e) the fractured surface of Sylgard/PCL composite.

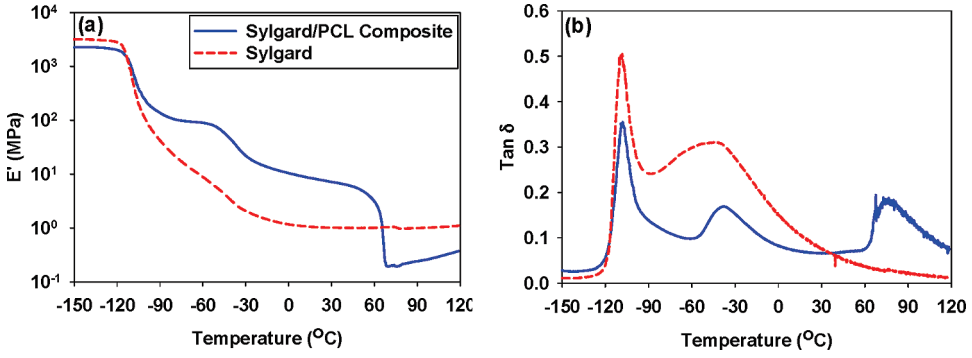

Figure 2. Dynamic mechanical analysis (DMA) of the Sylgard/PCL composite and neat Sylgard.

stretched at 80 °C (T > PCL T_m) by gradually ramping the tensile stress to 0.20 MPa (step 1), followed by cooling to 5 °C at a rate of 2 °C/min while holding the stress constant (step 2). The stress was then quickly released at 5 °C to witness strain fixing (step 3). The unconstrained strain recovery was triggered by heating to 80 at 2 °C/min (step 4). This thermomechanical cycle (steps 1−4), known as the "one-way shape memory (1WSM) cycle",[1,13,14] was then performed consecutively for two more times on the same sample. As can be observed, a large strain (ca. 95%) was retained (fixed) after unloading at 5 °C. In contrast, neat Sylgard showed no capability to fix strain; i.e., the strain diminished to zero as the stress was released at 5 °C. The Sylgard/PCL composite showed a sharp recovery centered at ∼60 °C, in accordance with the melting temperature of PCL (Figure 2). A large percentage of fixed strain was recovered while a permanent (unrecovered) strain of about 30% remained at 80 °C. The shape memory performance showed no deterioration over the three cycles performed, in that the curves are almost identical. While this suggests good cycle lifetime for the material, we are conducting more extensive cycling experiments for quantitative assessment.

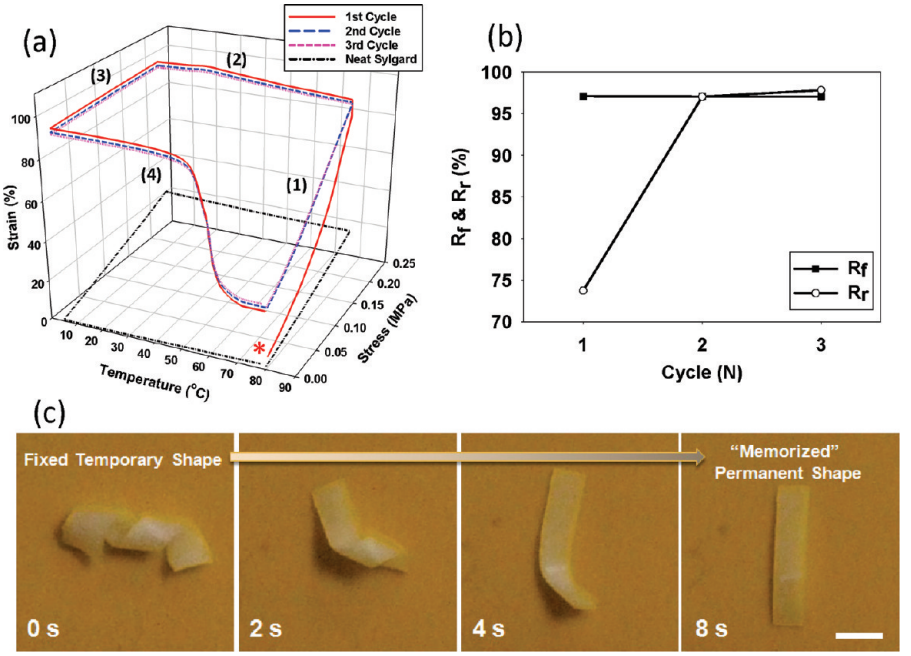

Figure 3. Shape memory properties of Sylgard/PCL SMECs. (a) Stress−temperature−strain plot showing the one-way shape memory (1WSM) cycles of Sylgard/PCL, compared with neat Sylgard (the asterisk indicates the onset point). (b) Fixing ratio (R_f) and recovery ratio (R_r) calculated for three cycles. (c) Photographs of Sylgard/PCL composite showing the recovery from a fixed temporary shape to its "memorized" permanent shape on a temperature-controlled plate at 80 °C (the scale bar represents 5 mm).

To further quantify the shape memory behavior, we calculated fixing ratio (R_f) and recovery ratio (R_r) according to[15]

$$R_f(N) = \frac{\varepsilon_u(N)}{\varepsilon_m(N)} \times 100\% \quad \text{and}$$

$$R_r(N) = \frac{\varepsilon_u(N) - \varepsilon_p(N)}{\varepsilon_u(N) - \varepsilon_p(N-1)} \times 100\%$$

where ε_m, ε_u, ε_p, and N represent the strain before unloading, the strain after unloading, the permanent (residual) strain after heat-induced recovery, and the cycle number, respectively. In both cases a value of 100% indicates complete strain fixing/recovery. For cycle 1, $\varepsilon_p(0)$ was taken as the initial strain (ca. 5%, primarily thermal strain) at the beginning of the experiment. The calculated R_f and R_r are shown in Figure 3b for all the three cycles. The Sylgard/PCL composite shows almost complete shape fixing, evident from a high R_f value ($>97\%$) that was almost unchanged through cycles 1−3. On the other hand, the recovery ratio R_r increased significantly from 73.8% in cycle 1 to 97.0% in cycle 2 and then slightly to 97.8% in cycle 3. This implies that, in practice, one can conduct a thermomechanical "conditioning" of the material (corresponding to cycle 1) to achieve high R_r in future uses, if complete shape recovery is desired in the given application.

Finally, a series of photographs were taken as a visual presentation of the shape recovery process (Figure 3c). The sample was preheated at 80 °C, wound around a cold glass rod, and allowed to cool. The shape recovery was then triggered by placing the shape-fixed (coiled) sample on a hot plate at 80 °C. The whole recovery process accomplished within several seconds, as shown.

To conclude, we have successfully developed a shape memory elastomeric composite (SMEC) using a unique approach. Besides the excellent shape memory performance and ease of fabrication, another obvious advantage of our approach is its versatility and broad applicability, since it requires no specific chemistry or physical interactions. One can tune the properties of the individual components (the fibers and the matrix) to easily control the overall shape memory behavior and materials properties. For example, one can use thermoplastic fibers (either semicrystalline or amorphous) with different T_m's and T_g's to adjust the transition temperature or vary the cross-link density of the matrix to achieve different recovery stresses. Given the pervasiveness of silicone rubber (indeed, Sylgard 184) in the field of microcontact printing and microfluidics, we anticipated innovations derived from the new SMEC materials in those fields. Our ongoing research on the new materials is focused on understanding the detailed structure−properties relationships in a variety of different SMEC systems.

Supporting Information Available: (1) Fiber diameter analysis of electrospun PCL fiber mat, (2) DSC thermograms of bulk PCL, electrospun PCL, and Sylgard/PCL composite, and (3) room temperature tensile stress−strain loading/unloading results of Sylgard/PCL composite to different final strains. This material is available free of charge via the Internet at http://pubs.acs.org.

References and Notes

(1) Mather, P. T.; Luo, X.; Rousseau, I. A. *Annu. Rev. Mater. Res.* **2009**, *39*, 445–471.
(2) Liu, C.; Qin, H.; Mather, P. T. *J. Mater. Chem.* **2007**, *17*, 1543–1558.
(3) Lendlein, A.; Kelch, S. *Angew. Chem., Int. Ed.* **2002**, *41*, 2034–2057.
(4) Mather, P. T. *Nat. Mater.* **2007**, *6*, 93–94.
(5) Rousseau, I. A.; Mather, P. T. *J. Am. Chem. Soc.* **2003**, *125*, 15300–15301.
(6) Weiss, R. A.; Izzo, E.; Mandelbaum, S. *Macromolecules* **2008**, *41*, 2978–2980.
(7) Osada, Y.; Matsuda, A. *Nature* **1995**, *376*, 219–219.
(8) Bergshoef, M. M.; Vancso, G. J. *Adv. Mater.* **1999**, *11*, 1362–1365.
(9) Jong-sang, K.; Darrell, H. R. *Polym. Compos.* **1999**, *20*, 124–131.
(10) Choi, J.; Lee, K. M.; Wycisk, R.; Pintauro, P. N.; Mather, P. T. *Macromolecules* **2008**, *41*, 4569–4572.
(11) Zhang, H.; Wang, H.; Zhong, W.; Du, Q. *Polymer* **2009**, *50*, 1596–1601.
(12) Mark, J. E. *Polymer Data Handbook*; Oxford University Press: New York, 1999.
(13) Chung, T.; Romo-Uribe, A.; Mather, P. T. *Macromolecules* **2007**, *41*, 184–192.
(14) Qin, H.; Mather, P. T. *Macromolecules* **2008**, *42*, 273–280.
(15) Rousseau, I. A. *Polym. Eng. Sci.* **2008**, *48*, 2075–2089.